Wave Energy Dissipation by Whitecaps

C. KRAAN, W. A. OOST, AND P. A. E. M. JANSSEN

Royal Netherlands Meteorological Institute, de Bilt, the Netherlands

9 December 1994 and 28 June 1995

ABSTRACT

With video equipment and image processing software the authors have measured the whitecap coverage of the sea surface near the Dutch coast. Reality proved the initial idea about the simplicity of this way of whitecap measurement to be overly optimistic. A model was developed that produces a theoretical estimate of the whitecap percentage as a function of the wave age, which in turn depends on the wave peak frequency and the friction velocity in the air. The comparison between the measured whitecap coverage and the model results shows an order of magnitude correspondence for most data. A group of outliers appears to be connected to the strength of the current.

1. Introduction

Whitecaps are a subject of increasing importance, both because of the role of wave breaking in energy dissipation of surface waves and because of the effects of the associated surface disruptions on air–sea transfer processes such as momentum, heat, or gas exchange. In 1986, the Humidity Exchange over the Sea (HEXOS) main experiment (e.g., Katsaros et al. 1987) took place at Meetpost Noordwijk (MPN), a research platform 9 km off the Dutch coast. During that experiment we made a number of video recordings of the water surface that were analyzed for whitecaps by Monahan (Monahan et al. 1988), who pioneered this method of obtaining information about breaking waves.

In 1993 the Air Sea Gas Exchange (ASGASEX) experiment took place, again at MPN. The primary subject of this project was the study of gas exchange at the sea surface, and in this connection we looked again into the possibilities, offered by present-day video technology, for automated whitecap detection.

Much has changed in this respect between 1986 and 1993. Personal computer video cards, allowing on-line digitization of video signals, have been commercially available now for a number of years. They scan and process video pictures in real time, that is, at a rate of 25 pictures per second. The data are stored as two-dimensional arrays (frames), each corresponding—for our equipment—to a picture resolved into 512 × 512 pixels. The values stored in each of these 262 144 memory positions represent the gray level (brightness) of the corresponding place in the picture. Software packages containing the basic procedures for handling and further processing of these digitized pictures are also commercially available. Our specific hardware consisted of a high-resolution frame grabber (DT2851), an auxiliary frame processor (DT2858), and an eight-channel video multiplexer (DT2859) all from Data Translation Inc. This firm also provided our software: a subroutine library DT-IRIS V01.04 that we used in combination with Microsoft Pascal 3.31.

The basic assumption for automatic whitecap detection is that the whitecaps in a video picture of the sea surface correspond to all pixels with a gray level above a certain threshold value and that all other elements in the picture have gray levels below that threshold. The whitecap percentage (WCP, the percentage of the sea surface covered with whitecaps) then follows directly from the ratio between the number of pixels with a gray level above the threshold and the total number of pixels.

Section 2 of the paper describes the technical setup of the experiment, and section 3 the method of data extraction. A fairly simple model of wave energy dissipation due to whitecaps is presented in section 4, and the output of the model is compared with the in situ whitecap measurements in section 5.

More information about whitecap phenomena can be found in, for example, Monahan and MacNiocaill (1986), Katsaros and Ataktürk (1992), and Banner and Peregrine (1993). For the technical details of image processing we refer to Gonzales and Woods (1992).

2. Equipment and mounting

During ASGASEX, we used two black-and-white video cameras. One camera (indicated as "WC," for whitecaps) was installed at the helideck, 18 m above

Corresponding author address: Dr. W. A. Oost, Royal Netherlands Meteorological Institute, P.O. Box 201, 3730 AE de Bilt, The Netherlands.

mean sea level. This camera had a remotely controlled pan and tilt facility and looked over the sea surface in a more or less horizontal plane. Its field of view was about 100 km^2. We assumed a homogeneous distribution of the whitecaps in the field of view of the camera. The diminishing contribution to the picture of areas farther away from the camera then does not affect the whitecap fraction, because the whitecap area in the picture is distorted in the same way as the remaining wave field.

The second camera ("BR," for breaking waves) was mounted on the instrument boom of the Royal Netherlands Meteorological Institute. When in use the boom was parallel to the sea surface; in that position the BR camera was looking straight down. The height of the boom above the water could be varied; at its mean height of 6 m, the observed area was 6 m × 9 m. The BR camera was intended to observe breaking wave events directly below the instrument boom.

All signals were registered on videotape. The whitecap percentage was calculated directly from the signal (on-line) as well as afterward from the registered signal (off-line). We consider the on-line results as inferior to the off-line ones because for the on-line data the gray-level threshold had to be estimated and set before the start of a recording and factors such as changes in the lighting, due to clouds or the position of the sun, may well have affected the on-line results.

The wind and wave data that we will use are, respectively, from a pressure anemometer (Oost et al. 1991) on the boom and from a Datawell waverider, moored some 150 m southwest of the platform.

Close to the BR camera a microphone was mounted, intended to detect whitecaps by recording and filtering the sound of wave breaking. These measurements are the subject of a separate paper.

3. Determining the whitecap percentage

We developed three software packages based on the DT-IRIS software specified in section 1. (DT-IRIS is merely a collection of basic commands to manipulate the video frames.) All three programs require an input value for the threshold level, the critical gray level above which the pixels are assumed to correspond only to whitecaps.

The whitecaps that we want to detect are the crests of breaking waves (type A, see Monahan 1969 or Monahan and Woolf 1989) and not the foam that a breaker leaves behind (type B), because only type A plays a part in the dissipation of wave energy. Determining the threshold is the most critical part of the processing: there is no objective criterion and often the foam just mentioned and/or the reflection of light at the sea surface do cause problems.

We tried to make our analysis as objective as possible by scanning the tape several times, using different thresholds, by avoiding areas in the pictures with strong reflections, and by using three different analysis methods.

In the first method, we straightforwardly calculated, for a selected threshold value of the gray level, the whitecap percentages as well as their progressive mean, for as many frames of a run as possible. This procedure was used for both on-line and off-line data. At a maximum we can calculate each second the WCPs of two frames; that is, 8% of the data offered to the system that produces its pictures at the usual speed of 25 Hz. The procedure was repeated with different threshold values until a gray level was found where the WCP varied very little with changes in the threshold. The WCPs in this range were considered the actual ones.

For the second approach we measure the WCP after subtracting, pixel by pixel, the gray-level values of two frames. This results in a new frame in which only pixels at positions where changes occurred have a value different from zero. The time lag between the pictures is adjustable. With this method we intended to eliminate the effects of foam, which is more or less stationary on the surface, whereas the whitecaps move with the velocity of the wave. With this second method we needed 2 s to calculate a WCP.

As an aside, we note that the difference between the results of the first and second method can be used to estimate the foam coverage, an idea we did not apply.

In the third approach we take the average of an adjustable number of frames and calculate the WCP of the result. Here again we needed 2 s for the calculation of a WCP.

The three methods give consistent results for a time lag of 0.4 s (in the second method) and for averaging over seven frames (with the third method).

All methods were applied on-line (directly) and off-line (on tape) and on data of both cameras. The results show a large scatter, but we found no systematic differences between cameras or methods.

The stability of the results of our three independent methods gives us the conviction that these results have physical significance. Whether the values we find are actually the areal percentages or fractions of type A, whitecaps cannot be determined as long as we have no generally accepted and straightforward method to determine that quantity. This study in fact was started on the assumption that automated video measurements provided such a method. Experience told us otherwise.

To further check the reproducibility of our analysis, we analyzed a number of times different areas of the same pictures, to see whether the resulting whitecap percentages were consistent. This turned out to be the case within 5%.

The data we present in this paper are off-line data (i.e., based on tape recordings, both of the WC and BR camera's), analyzed with the first approach.

In most cases the (area averaged) WC data agreed well with the (time averaged) BR data of the same run. Our runs lasted between 15 and 45 min, which is sufficiently short to assume stationarity of the situation. The area surveyed by the WC camera (which was always looking in an off-shore direction) furthermore may be considered homogeneous within the limits posed by the (in)accuracy of the method. The results show an rms error in the overall mean WCP of a run of 5%–10%, with the BR results somewhat higher than those from the WC camera. The best estimate of the overall accuracy is probably found by comparing the results of the three analysis methods, which shows differences of about a factor of 2.

The dynamic range of the tape registrations is clearly smaller than that of the on-line signal, so the on-line and off-line thresholds usually will be different.

4. Modeling the dissipation of wave energy by whitecaps

a. General

Using Monahan's (1969) freshwater results, Cardone (1969) already argued that whitecapping is directly related to the rate of energy dissipation from the wave field and that the percentage of the water "surface covered by whitecaps . . . is directly related to the rate of energy transfer from the air flow to the fully developed spectral components (of the waves). . . ." We start from the usual equation for the evolution of the wave variance spectrum (Komen et al. 1994):

$$\frac{DF}{Dt} = S_{in} + S_{nl} + S_{ds},$$

where F is the energy variance, S_{in} is the source term for the wind input, S_{nl} is for the nonlinear interaction between the waves, and S_{ds} is the energy dissipation. The last term covers dissipation by wave breaking, microscale breaking, and bottom friction (Banner and Peregrine 1993). Here we neglect both the microscale breaking and the bottom friction (the average local water depth is 18 m). The energy dissipation per unit time is given by

$$\epsilon_{ds} = \rho_w g \int S_{ds} d\omega \quad (\mathrm{W\ m^{-2}}) \tag{1a}$$

and, in normalized form (based on dimensional analysis),

$$\epsilon_{dsn} = \frac{\epsilon_{ds}}{\rho_a u_*^3}, \tag{1b}$$

with ρ_a and ρ_w the specific density of air and water, respectively, u_* the friction velocity, and ω the circular frequency of the wave.

b. Dissipation source function

The dissipation source function (effectively a sink) is given by Komen et al. (1984) and by the WAM group (1988) as

$$S_{ds} = -\beta\omega^2 F, \tag{2}$$

where

$$\beta = \frac{c_0}{\bar{\omega}}\left(\frac{\bar{\alpha}}{\bar{\alpha}_{\mathrm{PM}}}\right)^2,$$

with $c_0 = 3.35 \times 10^{-5}$ and $\bar{\alpha}_{\mathrm{PM}} = 4.57 \times 10^{-3}$. (The subscript PM indicates that this quantity originates from the Pierson–Moskowitz spectrum.)

If we assume for simplicity that the spectral function can be factored in a normalized frequency part $G(\omega)$ and a directional part $H(\theta)$ we can write for

the wave variance

$$E = \int G d\omega, \tag{3a}$$

the mean frequency

$$\bar{\omega} = \frac{1}{E}\int \omega G d\omega, \tag{3b}$$

and the integral wave steepness parameter

$$\bar{\alpha} = E\bar{\omega}^4 g^{-2}. \tag{3c}$$

c. Theoretical estimate of energy dissipation

The contribution of whitecaps to wave energy dissipation can be approximated in a simple way (see also Komen et al. 1994, p. 145) as

$$\epsilon_{ds} = -\gamma\rho_w g \mathrm{WCF}\omega_p E \quad (\mathrm{W\ m^{-2}}), \tag{4}$$

where γ in this expression is the average fraction of the total wave energy dissipated per whitecapping event. Its value has to lie between 0 and 1. WCF is the whitecap fraction (the fraction of the sea surface covered with whitecaps) and ω_p the (circular) peak frequency; $\bar{\omega} = c_1\omega_p$, where the c_1 coefficient depends on the definition of $\bar{\omega}$ and the spectral shape.

d. Calculation of WCF (theory)

We can find a theoretical expression for the WCF combining (1a), (1b), (2), and (4) into

$$\int \beta\omega^2 G d\omega = \gamma \mathrm{WCF}\omega_p E.$$

Using definition (3) and the expression for β, we find

$$\mathrm{WCF} = \frac{\beta\int \omega^2 G d\omega}{\gamma\omega_p E} \tag{5a}$$

$$= \frac{c_0 c_1}{\gamma}\frac{\int G d\omega \int \omega^2 G d\omega}{\left(\int \omega G d\omega\right)^2}\left(\frac{\bar{\alpha}}{\bar{\alpha}_{\mathrm{PM}}}\right)^2. \tag{5b}$$

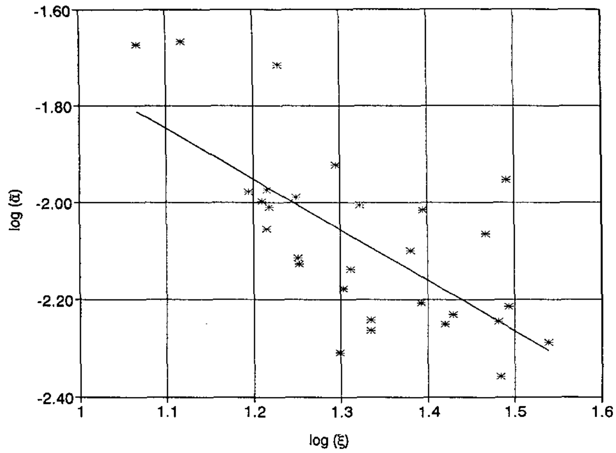

FIG. 1. Logarithmic plot of $\bar{\alpha} = 3.2\, H_s^2 f_p^4$ vs the measured values for the wave age $\xi = g/2\pi u_* f_p$. The (regression) line corresponds to $\bar{\alpha} = 0.2\xi^{-1.04}$.

e. Spectral shape

Measurements of the whitecap coverage show a large scatter. We found that we could approximate the measured spectra to an accuracy well within that of the whitecap percentages by the simple expression (WMO 1976, section 2.8)

$$G(\omega) = \begin{cases} \alpha g^2 \omega^{-5}, & \omega \geqslant \omega_p \\ 0, & \omega < \omega_p \end{cases}, \tag{6}$$

where α is the Phillips constant.
Integrating (6) over all frequencies, we find expressions for ω_p and $\bar{\omega}$ [the latter by using (3a) and (3b)], resulting in $c_1 = 4/3$. The right-hand side of (5b) becomes

$$\mathrm{WCF} = \frac{9}{8}\frac{c_0 c_1}{\gamma}\left(\frac{\bar{\alpha}}{\bar{\alpha}_{\mathrm{PM}}}\right)^2$$

or, substituting the values of $c0$, $c1$, and $\bar{\alpha}_{\mathrm{PM}}$,

$$\mathrm{WCF} = \frac{2.4}{\gamma}\bar{\alpha}^2. \tag{7}$$

With the expression for $\bar{\alpha}$ in mind, namely, $\bar{\alpha} = E\bar{\omega}^4/g^2$, it is clear that the results are very sensitive to the value of c_1 and so for the shape of the spectrum.

f. Determining $\bar{\alpha}$

During the video recordings we made simultaneous wind and wave measurements, so we know the significant waveheight H_s (m), the peak frequency f_p (Hz), and the atmospheric friction velocity u_* (m s^{-1}). These data make it possible to estimate $\bar{\alpha}$ as

$$\bar{\alpha} = E\bar{\omega}^4 g^{-2} = \frac{(2\pi c_1)^4}{16 g^2} H_s^2 f_p^4 = 3.2 H_s^2 f_p^4,$$

if we take $E = H_s^2/16$ and $\bar{\omega} = c_1\omega_p = 2\pi c_1 f_p$.

If we eliminate the fetch from the JONSWAP spectral formula (Hasselmann 1973), it appears appropriate to write $\bar{\alpha} = a\xi^b$, with $\xi = c_p/u_* = g/2\pi u_* f_p$ the wave age. We then find from a regression analysis (Fig. 1)

$$a = 0.20 \pm 0.02 \quad \text{and} \quad b = -1.04 \pm 0.2,$$

with a correlation of 69%.
So from the wind and wave measurements we find

$$\bar{\alpha} = 0.2\xi^{-1.04}, \tag{8}$$

which gives the wave steepness as a function of wave age. Comparable values for a and b are found in the literature; for example, Komen et al. (1994) give $a = 0.57$ and $b = -1.5$.

5. Comparing theory and field data

If we combine (7) and (8), the resulting expression gives us the whitecap percentage (WCP) as a function of the wave age. To compare these theoretical values with the field measurements we have to make an estimate of the fraction γ.

From Melville and Rapp (1985) we find, taking a value of 0.2 for the wave steepness in their Fig. 4, that whitecaps are responsible per event for the loss of about 10% of the total wave energy, so $\gamma = 0.1$. Then

$$\mathrm{WCP} = 100 \times \frac{2.4}{0.1}(0.2)^2 \xi^{-2.08} = 96\xi^{-2.08} \tag{9}$$

If we plot the measured WCP as a function of the wave age, we can compare the field data with the theoretical values based on (9) (Fig. 2). From the figure it is clear that theory and experiment give values of the same order of magnitude, although there is a large scatter in

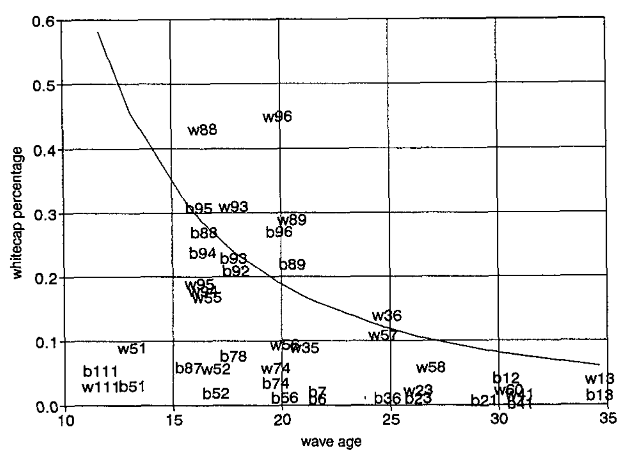

FIG. 2. Measured whitecap percentages of the sea surface vs measured wave age c_p/u_*. W*nn* are data measured with the whitecap, B*nn* data from the breaker camera, with *nn* indicating the run number. For reasons of clarity two points were left out (in this figure only): B35 is almost identical to B6 and W61 to W41. The line corresponds to Eq. (9).

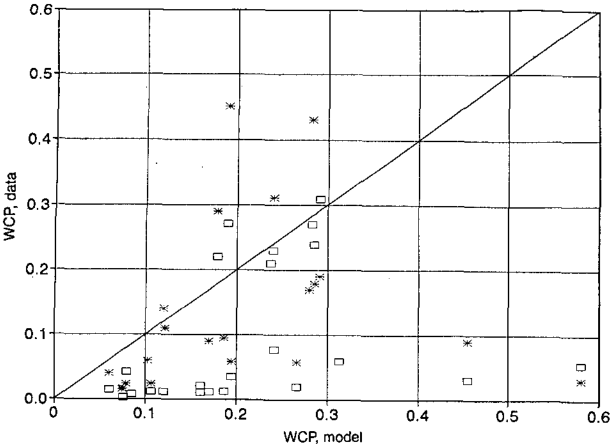

FIG. 3. Direct comparison between the modeled and measured whitecap percentages (WCPs). Asterisks—WC camera; squares—BR camera.

the experimental values. In Fig. 3 the same results are compared directly. The figure again shows that theory and experiment lead to whitecap percentages of the same order of magnitude.

No error bars are plotted in the figures, because it is difficult to estimate the error of the measured WCPs. The plotted values are averages per run and have, in general, a standard deviation of 5%–10%, due to variations in the WCP itself and changes in the circumstances during the run. Technically the measurement error is very small. The error in the model values is even more difficult to assess; section 4f gives some indication in this respect. If our assumptions about the homogeneity and stationarity of the whitecap phenomena during a run are correct, the scatter should mainly be caused by inadequacies of the measurement techniques used. The correlation coefficients between the modeled and measured whitecap percentages are 17% and 26% for the WC and the BR camera, respectively. These numbers are based on data produced with the first (direct) type of analysis method.

6. Special effects

Figures 2 and 3 give the impression that there are two different kinds of field data: one with a high (WCP $\approx 0.25\%$) and one with a low (WCP $\approx 0.05\%$) whitecap percentage. We therefore scrutinized our data to find a connection with other parameters.

By visual observation we had noted two situations where no whitecaps were visible, though the wind speed was in the range 7–8 m s^{-1}. In one of these instances the air–sea temperature difference was measured as 6°C (very stable), in the other case it was 0°C (near neutral), but on both occasions there was a strong tidal current (about 1 m s^{-1}). This suggested that the absence of the whitecaps was not caused by, for example, the atmospheric stability but by the current.

Inspired by these occurrences we plotted our WCP values against the speed of the (mainly tidal) current (Fig. 4). The plot indeed suggests a descending maximum value for the WCP as a function of the current velocity, with two exceptions, a WC and a BR value that belong to the same run. The figure is not very convincing, due to the limited number of data points. However, if we compare Figs. 2 and 4 we find the data points at high current velocities in Fig. 4 as the group with the low whitecap percentage at low values of the wave age in Fig. 2. A tentative conclusion therefore is that in these fairly shallow tidal waters the current speed puts an upper limit to the WCP value but that below this limit the wave age appears to be the determining factor. The mechanism through which the current affects the WCP is at the moment a matter of speculation. A possibility in this respect could be interaction of the current shear and the long waves, which both can extend over the full water depth (18 m) in the MPN area.

We have not been able to detect any relationship between the WCP values and wind direction, wave height, wave direction, angle between camera and wave direction, atmospheric stability, current direction, or the angle between waves and current.

7. Concluding remarks

Our initial idea that commercially available hardware and software could provide us with an easy way to monitor the whitecap coverage must be considered as fairly optimistic. The large scatter of the results is caused by effects due to foam and/or reflection of light from the sea surface, by the influence of the relative angle between camera and wave direction, and, possibly, by the effects of the current on the whitecaps.

A major obstacle was the determination of the threshold value. We have been able to develop a satisfactory method to solve this problem.

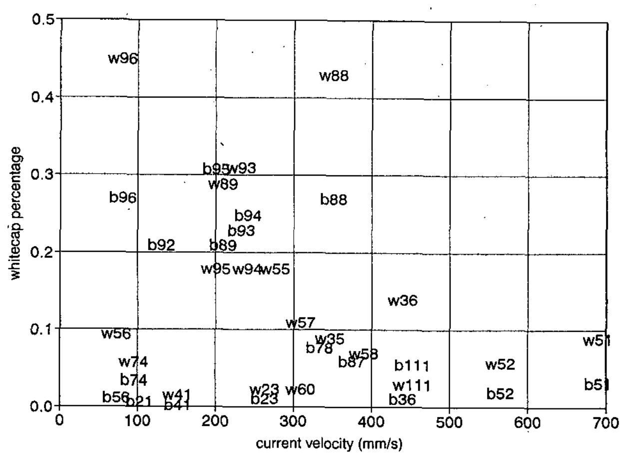

FIG. 4. The measured whitecap percentage as a function of the current velocity. Symbols as in Fig. 2.

Using this method we obtained results that agreed in order of magnitude with theory, which allowed us to make a first assessment of a model expression for the whitecap coverage.

The results showed indications for effects of the current speed on the WCP. We want to stress that these effects should have a high priority in further research in this field because they may well be more important than those due to, for example, stability.

Acknowledgments. We would like to thank Gerbrand Komen for his advice and comments. Assistance with instruments, data, hardware and software by Cor van Oort, Hendrik Wallbrink, and Ed Worrell is sincerely appreciated. Finally our thanks to Mrs. Elly van Duivenbooden for typing the initial version of the manuscript. We thank the reviewers of the paper for their remarks, which led to some substantial improvements.

REFERENCES

Banner, M. L., and D. H. Peregrine, 1993: Wave breaking in deep water. *Ann. Rev. Fluid Mech.*, **25**, 373–397.

Cardone, V. J., 1969: Specification of the wind distribution in the marine boundary layer for wave forecasting. Tech. Rep. GSL-69-1, New York University, 131 pp.

Gonzales, R. C., and R. E. Woods, 1992: *Digital Image Processing.* Addison-Wesley, 716 pp.

Hasselmann, K., and Coauthors, 1973: Measurements of wind-wave growth and swell decay during the Joint North Sea Wave Project (JONSWAP), *Dtsch. Hydrog. Z.*, **A12** (Suppl.), 95 pp.

Katsaros, K. B., and S. S. Ataktürk, 1992: *Breaking Waves.* Plenum, 119–133.

——, S. D. Smith, and W. A. Oost, 1987: HEXOS—Humidity Exchange over the Sea, a program for research on water-vapor and droplet fluxes from sea to air at moderate to high wind speeds. *Bull. Amer. Meteor. Soc.*, **68**, 466–476.

Komen, G., S. Hasselmann, and K. Hasselmann, 1984: On the existence of a fully developed wind-sea spectrum. *J. Phys. Oceanogr.*, **14**, 1271–1285.

——, L. Cavaleri, M. Donelan, K. Hasselmann, S. Hasselmann, and P. A. E. M. Janssen, 1994: *Dynamics and Modelling of Ocean Waves.* Cambridge University Press, 532 pp.

Melville, W. K., and R. J. Rapp, 1985: Momentum flux in breaking waves. *Nature,* **317**, 514–516.

Monahan, E. C., 1969: Fresh water whitecaps. *J. Atmos. Sci.*, **26**, 1926–1929.

——, and G. MacNiocaill, Eds., 1986: *Ocean Whitecaps and Their Role in Air–Sea Exchange Process.* Reidel, 294 pp.

——, and D. K. Woolf, 1989: Comments on "Variations of whitecap coverage with wind stress and water temperature." *J. Phys. Oceanogr.*, **19**, 706–709.

——, M. B. Wilson, and D. K. Woolf, 1988: HEXMAX whitecap climatology: Foam crest coverage in the North Sea, 16 October–23 November 1986. *Humidity Exchange over the Sea Main Experiment (HEXMAX); Analysis and Interpretation,* W. A. Oost, S. D. Smith, and K. B. Katsaros, Eds., Tech. Rep., Dept. of Atmos. Sciences, AK-40, University of Washington, 105–115.

Oost, W. A., E. H. W. Worrell, J. W. Schaap, C. van Oort, and C. Kraan, 1991: An improved version of the pressure anemometer. *J. Atmos. Oceanic Technol.*, **8**, 331–340.

Smith, S. D., K. B. Katsaros, W. A. Oost, and P. G. Mestayer, 1990: Two major experiments in the Humidity Exchange over the Sea program. *Bull. Amer. Meteor. Soc.*, **71**, 161–172.

WAMDI Group (Wave Model Development and Implementation Group), 1988: The WAM model—A third generation ocean wave prediction model. *J. Phys. Oceanogr.*, **18**, 1775–1810.

WMO, 1976: *Handbook on Wave Analysis and Forecasting.* World Meteorological Organization,